Polyamines Accelerate Codon Recognition by Transfer RNAs on the Ribosome

ARTICLE *in* BIOCHEMISTRY · AUGUST 2010

Impact Factor: 3.02 · DOI: 10.1021/bi1009776 · Source: PubMed

6 AUTHORS, INCLUDING:

Byron Hetrick
University of Oregon
7 PUBLICATIONS **51** CITATIONS

SEE PROFILE

Published in final edited form as:
Biochemistry. 2010 August 24; 49(33): 7179–7189. doi:10.1021/bi1009776.

Polyamines Accelerate Codon Recognition by Transfer RNAs on the Ribosome

Byron Hetrick, **Prashant K. Khade**, **Kristin Lee**, **Jenise Stephen**, **Alex Thomas**, and **Simpson Joseph**
Department of Chemistry and Biochemistry, University of California, San Diego, 9500 Gilman Drive, La Jolla, CA 92093-0314.

Abstract

The selection of aminoacyl-tRNAs by the ribosome is a fundamental step in the elongation cycle of protein synthesis. tRNA selection is a multistep process that ensures only correct aminoacyltRNAs are accepted, while incorrect aminoacyl-tRNAs are rejected. A key step in tRNA selection is the formation of base pairs between the anticodon of the aminoacyl-tRNA and the mRNA codon in the A site, called “codon recognition”. Here, we report the development of a new, fluorescence-based, kinetic assay to monitor codon recognition by the ribosome. Using this assay we show that codon recognition is a second-order binding step under optimal conditions. Additionally, we show that at low Mg^{2+} concentration, the polyamines spermine and spermidine stimulate codon recognition by the ribosome without loss of fidelity. Polyamines may accelerate codon recognition by altering the structure and dynamics of the anticodon arm of the aminoacyl-tRNA.

Keywords

Ribosome; elongation factor Tu; decoding; translation

In all living organisms ribosomes decode the information in the mRNA to synthesize the corresponding polypeptide. During this process, the ribosome binds a ternary complex consisting of an aminoacyl-tRNA, an elongation factor (elongation factor Tu in *E. coli*) and a GTP to the A site. The cognate ternary complex is rapidly accommodated into the ribosome and participates in peptidyl transfer, while near-cognate and non-cognate ternary complexes fail to be accommodated and are rejected. This process is called tRNA selection and has to be sufficiently accurate in order to synthesize functional proteins. The error rate of translation in vivo has been estimated to be on the order of 10^{-3} to 10^{-4} (1,2). However, the difference in the free energy of binding between cognate and some near-cognate aminoacyl-tRNAs are small and does not explain how this high level of fidelity is achieved during protein synthesis.

The high fidelity of protein synthesis can be explained by a network of ribosome contacts that recognize the cognate codon-anticodon complex and by a conformational change in the decoding center of the ribosome. Structural studies revealed that the universally conserved bases G530, A1492 and A1493 in 16S rRNA precisely monitor the geometry of the codon-

Correspondence to: Simpson Joseph 4102 Urey Hall, Department of Chemistry and Biochemistry, University of California, San Diego, 9500 Gilman Drive, La Jolla, CA 92093-0314. Phone: (858) 822-2957 Fax: (858) 534-7042 sjoseph@ucsd.edu.

Supporting Information Available
Figures showing the effect of spermidine and Mg^{2+} on the binding of tRNAs to the ribosome, and representative time course of GTP hydrolysis and peptidyl transferase reaction. This material is available free of charge via the Internet at http://pubs.acs.org.

anticodon helix in the 30S subunit decoding center (3). These interactions are first established when the ternary complex binds to the ribosome (in the A/T state) and persist even after the aminoacyl-tRNA has been fully accommodated into the A site (in the A/A state) (4-6). The codon-anticodon base pairs in the A site trigger a conformational change in the ribosome called “domain closure” that is proposed to play a key role in accepting the cognate aminoacyl-tRNA (7). In contrast, near-cognate and non-cognate aminoacyl-tRNAs have mismatches between the codon and the anticodon that distorts the helix backbone and fail to establish proper interactions with G530, A1492, and A1493. Domain closure is then inhibited and the near-cognate and non-cognate aminoacyl-tRNAs are preferentially rejected by the ribosome. While these structural data nicely explain the molecular basis for recognition of the cognate aminoacyl-tRNA by the ribosome, kinetic studies are essential for understanding how the components of this process are orchestrated to incorporate the cognate aminoacyl-tRNA on a timescale that is compatible with the rate of protein synthesis in the cell.

A “kinetic proofreading” mechanism that explains how the ribosome improves the fidelity of tRNA selection was proposed independently by Hopffield and Ninio more than three decades ago (8,9). In accordance with this hypothesis, the ribosome carries out tRNA selection in two distinct stages that are separated by the irreversible hydrolysis of GTP by EF-Tu. The first selection stage is called “initial selection” and the second selection stage is called “proofreading”. During initial selection, cognate and near-cognate ternary complexes bind to the ribosome and trigger GTP hydrolysis on EF-Tu. In contrast, non-cognate ternary complexes dissociate rapidly from the ribosome before triggering GTP hydrolysis on EF-Tu. During proofreading, the cognate aminoacyl-tRNA is accommodated into the 50S subunit A site, while near-cognate aminoacyl-tRNAs are rejected. If GTP hydrolysis and petidyl transferase rates are sufficiently slow relative to the dissociation of incorrect ternary complexes, then the overall fidelity of tRNA selection will be equal to the product of the fidelity of the initial selection and proofreading stages. Thompson and colleagues experimentally confirmed the kinetic proofreading hypothesis (10-12). They showed that non-cognate ternary complexes are rejected prior to GTP hydrolysis (initial selection). In contrast, near-cognate ternary complexes could pass through initial selection and induce GTP hydrolysis over background. However, they are efficiently rejected prior to peptide bond formation (proofreading). The rates of GTP hydrolysis and peptide bond formation were considered to occur at the same rate for both correct and incorrect ternary complexes. Therefore, the increased dissociation rates of non-cognate ternary complexes before GTP hydrolysis and of near-cognate ternary complexes after GTP hydrolysis were proposed to be the basis for discrimination.

A more detailed kinetic model for tRNA selection was developed by Rodnina and co-workers, who performed pre-steady state kinetic analysis with fluorescently labeled tRNAs and GTP analogs (13,14). They identified many new steps in the tRNA selection pathway as illustrated in Figure 1. These studies showed that the forward rates of GTP hydrolysis and tRNA accommodation are accelerated for cognate ternary complex compared to near-cognate ternary complex suggesting an induced fit mechanism for tRNA selection. A salient feature of this kinetic scheme is the codon-independent formation of an initial complex by the ternary complex on the ribosome called “initial binding” (step 1 in Figure 1) (15). The initial binding step is common for cognate, near-cognate, and non-cognate ternary complexes and has been debated in the literature because this step may reduce the rate of protein synthesis due to competition for a common binding site on the ribosome (16,17).

The kinetic scheme for tRNA selection was largely confirmed by recent single molecule fluorescence resonance energy transfer (smFRET) studies (18-21). The smFRET experiments identified several distinct FRET states as the tRNA progresses through the

selection process consistent with the kinetic scheme proposed by Rodnina and co-workers (13,14). Additionally, smFRET studies revealed transient binding events by cognate and near cognate tRNAs, which were interpreted to be rapid sampling of the A site codon by the ternary complex (21). However, smFRET was unable to detect codon-independent binding of the ternary complex to the ribosome (initial binding) likely due to the large distance between the donor and acceptor dyes (18,21).

Here, we show that under optimal conditions, codon recognition is a second-order binding step followed by a first-order conformational change that we tentatively assign as domain closure. Furthermore, we show that at low Mg^{2+} concentration, polyamines significantly accelerate the codon recognition step of tRNA selection without loss of fidelity. Polyamines are known to bind to the anticodon arm of tRNA (22,23), which may stabilize the proper conformation required for rapid interaction with the A site codon.

Experimental Procedures

Buffers

Buffer for initial control reactions consisted of 20 mM Hepes-KOH (pH 7.6), 6 mM $MgCl_2$ 150 mM NH_4Cl, 4 mM 2-mercaptoethanol, 0.05 mM spermine, 2 mM spermidine (24). Buffer A consists of 50 mM Tris-HCl (pH 7.5), 70 mM NH_4Cl, 30 mM KCl, 3.5 mM $MgCl_2$, 0.5 mM spermidine, 8 mM putrescine, and 2 mM DTT (25). Buffer B consists of 50 mM Tris-HCl (pH 7.5), 70 mM NH_4Cl, 30 mM KCl, 3.5 mM $MgCl_2$, 0.5 mM spermine, 8 mM putrescine, and 2 mM DTT. Buffer C consists of 50 mM Tris-HCl (pH 7.5), 70 mM NH_4Cl, 30 mM KCl, 3.5 mM $MgCl_2$, 5 mM spermidine, 8 mM putrescine, and 2 mM DTT. Buffer D consists of 50 mM Tris-HCl (pH 7.5), 70 mM NH_4Cl, 30 mM KCl, and 20 mM $MgCl_2$ (26).

Ribosomes, mRNA, tRNAs, EF-Tu

Tight coupled 70S ribosomes used in all fluorescence experiments were isolated from *E. coli* MRE600 cells, essentially as described (27). Ribosomes used in GTP hydrolysis, peptidyl transfer and fidelity measurements were additionally purified by sucrose cushion as described (28). mRNAs 5 ’-AAGGAGGUAAAAAUGUUUGCU-3 ’ and 5 ’-AAGGAGGUAAAAAUGCUCGCU-3’ with a 3’-amino-modifier were purchased from Dharmacon and labeled with pyrene succinimide as previously described (29). The A site codon is underlined. All experiments were performed with pyrene-labeled mRNAs. $tRNA^{fMet}$ was purchased from Sigma.

E. coli $tRNA^{Phe}$ was purified as described previously (30). The final pellets were resuspended in water and $tRNA^{Phe}$ was further purified on a C18 column as previously described (31).

EF-Tu was purified using the IMPACT-CN system according to the supplier's protocol (New England Biolabs). Column buffer used also contained 30 μM GDP. The purity of EF-Tu was assessed by SDS-PAGE and coomassie staining. One band could be seen corresponding to EF-Tu and a second band corresponding to EF-Ts. EF-Ts was identified by molecular weight and functionally by the fact that GDP with Mg^{2+} could remove the protein from the EF-Tu purification. The concentration of EF-Tu was determined by the bradford assay. The activity of EF-Tu was assessed using a native gel assay for tRNA binding (32).

Nucleotid-free EF-Tu was purified using the same method as above with a few modifications. After passing the cleared lysate over the chitin column, the beads were first washed with column buffer containing no EDTA and incubated for 1 hour to remove EF-Ts. The column was then washed with column buffer containing no $MgCl_2$ and incubated for 1

hour to remove GDP. Cleavage buffer was then passed over the column and the purification proceeded exactly as above.

Ternary complex formation

Ternary complexes were formed by combining 1 mM phenylalanine, 3 mM ATP, 1 mM GTP, 3 mM phosphoenol pyruvate, 0.25 mg/mL pyruvate kinase, 3% phenylalanyl-tRNA synthetase, 15 μM EF-Tu, and 5 μM $tRNA^{phe}$ in the buffer to be used for each experiment and incubated at 37 °C for 1 hour. Ternary complexes were then diluted down to the working concentration for each experiment. The concentration of ternary complex was taken to be the concentration of tRNA in the reaction.

Initiation complex formation

Initiation complexes were formed by heat activating 0.25 μM tight-coupled 70S ribosomes at 42 °C for 10 min. Ribosomes were then cooled to 37 °C for 10 min. 0.33 μM pyrene labeled mRNA was added and incubated for 10 min. at 37 °C. 0.5 μM $tRNA^{fMet}$ was then added and incubated at 37 °C for 30 min. For experiments in buffers A, B, and C, initiation complexes were formed in 7 mM Mg^{2+} then diluted to the working Mg^{2+} concentration with magnesium free buffer.

Fluorimeter experiments

Fluorescence emission scans were performed with a Fluoromax-P (J. Y. Horiba, Inc. USA) using an excitation and emission bandpass of 1 nm. Samples were excited at 343 nm and emission scans from 360 to 420 nm were taken before and after the addition of ternary complex or ASL.

Stopped-flow measurements

Stopped-flow measurements were performed at 25 °C with a stopped-flow instrument (μSFM-20, BioLogic). The samples were excited at 343 nm (band pass 10 nm) and the fluorescence emission was measured after passing a longpass filter 361 AELP (Omega Optical, VT, USA) installed in front of the detector. 0.25 μM (final concentration) initiation complex was mixed with varying amounts ternary complex. Time courses of ternary complex binding were fit to the double exponential function: $Y = b + C1*\exp(-k1*x) + C2*\exp(-k2*x)$.

GTP hydrolysis

Measurements of GTP hydrolysis were performed essentially as described previously (33). Ternary complexes were incubated at 37 °C for 5 minutes using nucleotide-free EF-Tu (purified as described above). Time courses were performed with a quench flow (μQFM-400, BioLogic). Free phosphate was analyzed by PEI-cellulose TLC in 0.5 M potassium phosphate (pH 3.5). The extent of hydrolysis was quantified by a phosphorimager (Bio-Rad).

Peptidyl transferase assay by quench-flow

Peptidyl transferase reactions were performed in buffer A. Initiation complexes were prepared in buffer A (7mM Mg^{2+}) by incubating activated 70S ribosome (0.5 μM) with mRNA (0.75 μM) at 37 °C for 10 min. f[^{35}S]Met-$tRNA^{fMet}$ charging mixture prepared in buffer A (0.6 μM $tRNA^{fMet}$, 3 mM ATP, 0.7 μM [^{35}S]L-Methionine, 0.4 mM N^{10}-formyltertahydrofolic acid, 10 μg formyl transferase and 10 μg MetRS incubated at 37 °C for 20 min) was added directly to the ribosome-mRNA complex and the incubation was continued at 37 °C for 10 min. Unbound f[^{35}S]Met-$tRNA^{fMet}$ was removed by ultra-filtration using Microcon Centrifugal Filter Devices (Amicon; 100,000 MWCO) and by

washing two times with 300 μl of buffer A (7mM Mg^{2+}). The initiation complexes were recovered after washing and the concentration of Mg^{2+} was adjusted to 3.5 mM by adding buffer A lacking Mg^{2+}. To prepare EF-Tu•GTP•Phe-$tRNA^{Phe}$ ternary complex, EF-Tu•GTP was formed by incubating 1 mM GTP, 3 mM phosphoenol pyruvate, 2.5 μg/μl of pyruvate kinase, and 3 μM EF-Tu at 37 °C for 20 min in buffer A. Phe-$tRNA^{Phe}$(1.5 μM) was then added and the incubation was continued for another 20 min. To determine the rate of peptidyl transferase reaction 15 μl of 70S initiation complex was rapidly mixed with 15 μl of ternary complex and quenched with 1M KOH in a quench-flow instrument (μQFM-400, Bio-Logic). Diepeptide was resolved by electrophoresis on cellulose TLC plates and quantified using a phosphorimager (31). Similar procedure was followed for experiments in buffer B.

Fidelity Experiment

Initiation complexes were prepared as described above for peptidyl transferase assay by incubating activated 70S ribosome (0.5 μM), mRNA (0.75μM) and f[^{35}S]Met-$tRNA^{fMet}$ (0.75μM). Ternary complex was prepared as described above except EF-Tu and total tRNA concentrations were 300 μM and 200 μM, respectively. *E. coli* total tRNA (Sigma) was aminoacylated by S-100 extract and purified by phenol and chloroform extractions. Aminoacylated tRNAs were ethanol precipitated and stored in 10 mM sodium acetate (pH 5.2) and used for ternary complex formation. To determine the fidelity of tRNA selection, 10 μl of 70S initiation complex (0.5 μM) was mixed with 10 μl of ternary complex (200 μM) for 30 seconds and quenched with 0.1 M KOH. Dipeptides (f[^{35}S]Met-Phe and f[^{35}S]Met-Leu) were resolved by electrophoresis on cellulose TLC plates and quantified using a phosphorimager (Bio-Rad) (31). The extent of misincorporation was estimated by calculating the ratio of f[^{35}S]Met-Leu / f[^{35}S]Met-Phe + f[^{35}S]Met-Leu.

Results

Fluorescence based method to monitor tRNA binding to the A-site

In order to study the binding of aminoacyl-tRNA•EF-Tu•GTP ternary complex to the ribosome, we developed a fluorescence-based method utilizing a short model mRNA labeled at the 3' end with pyrene. Similar fluorescently labeled mRNAs have been used previously to study EF-G catalyzed translocation (29), mRNA binding to the 30S subunit (34), and RF1 recognition of stop codons (35). Ribosome initiation complexes (IC) were formed by sequentially adding the fluorescently labeled mRNA and initiatior $tRNA^{fMet}$ to heat activated tight-coupled ribosomes. Addition of ternary complex containing $tRNA^{Phe}$ to fluorescently labeled IC resulted in an increase in the fluorescence emission intensity of the pyrene probe (Figure 2B). Based upon crystal structures of the ribosome, the probe is located between the head and shoulder regions of the 30S subunit approximately 25Å from the center of the codon in the A-site (Figure 2A) (36). Therefore, direct interaction between the tRNA and the probe appear unlikely. The increase in fluorescence may be due to solvent exclusion by the bound A site tRNA and/or reduced mobility of the probe after codon-anticodon base pair formation.

EF-Tu mediated binding of tRNAs to the ribosome is a multistep process (Figure 1), therefore, it is necessary to understand what events in this process cause the observed fluorescence change (13). The H84A mutant of EF-Tu is deficient in GTP hydrolysis (37,38). Interaction of ternary complex containing H84A EF-Tu with fluorescently labeled IC resulted in the same increase in fluorescence as when ternary complex containing wild type EF-Tu bound to fluorescently labeled IC (Figure 2C). The equivalent increase in fluorescence in the absence of GTP hydrolysis indicated that an event that occurs prior to GTP hydrolysis or independently of GTP hydrolysis is the cause of the fluorescence change.

The same increase in fluorescence was also observed when a free tRNA bound to the A-site, indicating that the fluorescence change is not caused by an EF-Tu dependent step (data not shown). According to the current model for the binding of ternary complex to the ribosome, codon recognition is the most probable event causing the observed fluorescence change. To test if codon recognition causes the increase in fluorescence, anticodon stem loop analogs (ASL) of tRNAs were added to fluorescently labeled IC. An increase in the fluorescence intensity of pyrene was observed when ASL bound to the A-site however, the observed increase in fluorescence was not as large as when ternary complex bound to the ribosome, indicating that codon recognition is responsible for at least part of the observed fluorescence change (Figure 1D). Subsequent conformational changes of the ribosome complex may be responsible for the remaining fluorescence increase.

Effect of polyamines on ternary complex binding

Polyamines have a positive effect on the efficiency of in vitro protein synthesis (39). In addition, magnesium is commonly used to improve translation. However, higher-than-physiological concentrations of magnesium decrease the fidelity of protein synthesis (40-43). We have examined the effect of the polyamines spermine, spermidine and the effect of Mg^{2+} ions on the association of cognate and near-cognate ternary complexes to the ribosomal A-site. Cognate ternary complexes were mixed with fluorescently labeled ICs that have a UUU codon in the A-site, in buffers containing varying concentrations of spermine. As the concentration of spermine was increased, the rate of the fluorescence change increased until the complete fluorescence change had occurred before the first measured time point (Figure 3A). The effect of spermine appeared to be saturated at 0.5 mM although, because the complete fluorescence change had occurred within 10 seconds, higher concentrations could have a greater effect that was not observable. When ternary complexes were added to ribosomes programmed with the near-cognate codon CUC in the A-site, increasing concentrations of spermine appeared to have a similar effect (Figure 3B). A spermine concentration above 0.5 mM again appeared to saturate the rate of fluorescence change, however, the fluorescence change occurred more slowly and intermediate time points could be measured. These results agree well with the content of spermine in cells, which has been measured to be approximately 1 mM (Table 1) (44). These experiments were performed with an excess of wild type EF-Tu•GTP•Phe-$tRNA^{Phe}$ ternary complex. Therefore, the slow increase in fluorescence with the near-cognate CUC codon is due to multiple binding and rejection events before accommodation of the tRNA in the A site.

Similar experiments were performed varying the concentrations of another common polyamine, spermidine. Increasing the concentration of spermidine in the ternary complex binding reactions had a similar effect to spermine. However, the improvement in binding appeared to require a higher concentration of 2.5 mM to reach saturation (Figures S1A and S1B). This is consistent with the higher physiological concentration of spermidine of approximately 7 mM in *E. coli* (Table 1) (44). Mg^{2+} also stimulated the binding of ternary complex to the ribosome. However, in the case of near-cognate ternary complex, the improvement in binding does not saturate even with 20 mM Mg^{2+} (Figures S1C and S1D).

Kinetics of ternary complex binding to the A-site

To understand how polyamines affect tRNA binding to the ribosome, we measured the kinetics of ternary complex binding to the ribosome in a stopped-flow fluorimeter. Four reaction conditions were tested: buffers A, B, C, and D (Table 1). Buffer A, B, and C all contained a low Mg^{2+} concentration of 3.5 mM previously used to study high fidelity tRNA selection by the ribosome (25). Buffer A also contained 0.5 mM spermidine, a concentration much lower than physiologically present (44). Buffer B contained 0.5 mM spermine, which appeared to greatly stimulate tRNA binding in the above experiments and is near the

physiologically present concentration of approximately 1 mM (44). Buffer C contained 5 mM spermidine, which also stimulated binding of tRNAs and is near the physiologically present concentration of approximately 7 mM in *E. coli* (44). Buffer D contained 20 mM Mg^{2+} and did not contain any polyamines. Buffers A and D (correspond to HiFi and LoFi, respectively) have previously been used to study the detailed mechanism of tRNA discrimination by the ribosome (26).

Ternary complexes were mixed with fluorescently labeled IC in a stopped-flow fluorimeter to measure the time course of fluorescence change. H84A EF-Tu was used to form ternary complexes in order to simplify the data analysis, as H84A EF-Tu does not hydrolyze GTP on the time scale of these experiments. In all four buffer conditions, a biphasic increase in fluorescence was observed (Figure 4A). Stopped-flow time courses were fit to the sum of two exponential equations to determine the observed reaction rates of each phase. The observed rates of the fluorescence change were significantly faster in buffers B, C and D relative to A, indicating that polyamines stimulate the binding of ternary complex to the ribosome as well as 20 mM Mg^{2+}. Time courses of wild type EF-Tu ternary complex binding appeared identical to H84A EF-Tu ternary complex.

To determine the association rate constant of ternary complex binding to the ribosome, we performed the experiment with 0.25 μM fluorescently labeled IC and varying concentrations of ternary complex. Plotting the observed rate of the first phase against ternary complex concentration showed a linear concentration dependence in buffers B, C and D (Figure 4B). A linear concentration dependence indicates a second order reaction where the slope of the line is equal to the second-order association rate constant (Johnson 1986). The association rate constant of ternary complex binding to the ribosome was 84 μM^{-1} s^{-1} in buffer B and 86 μM^{-1} s^{-1} in buffer C indicating that the polyamines spermine and spermidine stimulate the binding of ternary complex to the ribosome equivalently at their respective physiological concentrations (Table 2). In buffer D, the association rate constant was 66 μM^{-1} s^{-1} indicating that the polyamines can stimulate the binding of ternary complex to the ribosome at least as well or slightly better than even 20 mM Mg^{2+}. The association rate constant of ternary complex binding to the ribosome measured here is in good agreement with previous measurements using a different fluorophore (13). In buffer A, a hyperbolic relationship between the observed rate of the first phase and ternary complex concentration that saturated at a rate of 5 s^{-1} was observed (Figure 4C and Table 2). A hyperbolic concentration dependence indicates that a first-order conformational change is rate limiting (45). The slow rate of binding observed here is quite different from previous measurements of ternary complex association to the ribosome in the same buffer system (25). Differences in the rate of binding could potentially be attributed to the fact that in our measurements, the ternary complex was not purified. The higher NTPs would result in less free Mg^{2+} even though the total Mg^{2+} content of the reactions is the same. More importantly, physiological concentrations of either spermine, spermidine or high concentrations of Mg^{2+} were able to stimulate the binding of ternary complex to the ribosome.

The concentration dependence of the second phase of the stopped-flow time courses showed a hyperbolic concentration dependence under all conditions tested, consistent with a first-order conformational change (Figure 4D). The rate of this conformational change is much faster in the presence of higher concentrations of spermine, spermidine or Mg^{2+}. The second step saturated at rates of 2.3 s^{-1} in buffer B, 2.7 s^{-1} in buffer C, and 2.4 s^{-1} in buffer D. In buffer A, the second phase saturated at a significantly lower rate of 0.2 s^{-1} (Table 2).

Domain closure in ternary complex binding

Biphasic kinetics often result from a two step sequential mechanism where the receptor and ligand first collide in a second-order association step then undergo a conformational change

to form the final, tightly bound, complex (46). However, other binding mechanisms may also result in biphasic kinetics. For example, if one binding partner isomerizes between an active and inactive binding conformation, the active population will immediately bind while the inactive population must first isomerize to the active conformation before binding. If the isomerization step is relatively slow, biphasic-binding kinetics will be observed (47). Additionally, multiple binding pathways may exist that exhibit different reaction kinetics. In order to differentiate among the above mechanisms, we plotted the fraction of fluorescence change contributed by each phase of the stopped-flow time courses versus ternary complex concentration (Figure 5A). Under all conditions tested, approximately 75% of the total fluorescence change observed could be attributed to the first phase and 25% could be attributed to the second phase of the fluorescence change (Figure 5A). The amplitude of each phase did not change as the concentration of ternary complex was increased. The constant amplitudes of each phase supports a two step binding mechanism rather than an isomerization of ternary complex or multiple active populations of ternary complex as the cause of biphasic stopped-flow time courses. If isomerization or multiple populations of ternary complex caused biphasic kinetics, it would be expected that the fast phase of the stopped-flow time courses would contribute more of the fluorescence change as the concentration of ternary complex is increased because the faster binding variants of ternary complex would quickly bind all available sites, preventing the slower population from binding. Isomerization of the ribosome, or multiple binding pathways due to subpopulations of ribosomes cannot be completely excluded based on this data. However, kinetics of GTP hydrolysis and peptidyl transfer (see below) indicate that subpopulations of ribosomes are not responsible for the biphasic time courses.

Consistent with a two step binding mechanism associated with the biphasic stopped-flow time courses, control reactions indicate that codon recognition followed by domain closure of the 30S subunit are the causes of the observed fluorescence change. When ternary complex binds to fluorescently labeled IC, a ~ 30% increase in fluorescence occurs (Figure 5B). As previously described, a smaller increase in fluorescence of ~ 20% occurs when ASL binds to the A-site of the ribosome. Crystal structures of the 30S subunit with an ASL bound in the presence and absence of the miscoding antibiotic paromomycin revealed a conformational change known as domain closure where the head and shoulder of the 30S subunit rotate inwards, toward the decoding center (7). Although cognate ASL induces domain closure, the extent of domain closure is greater in the presence of both cognate ASL and paromomycin (7). Based upon the location of the probe, we hypothesized that the fluorescent probe could be sensitive to domain closure of the 30S subunit. Consistent with observations of domain closure from crystal structures, the full fluorescence change was observed when ASL bound to the ribosome in the presence of paromomycin (Figure 5B). Since a saturating concentration of ASL (20 μM) was used in these experiments, the increase in fluorescence is not due to increased binding of the ASL in the presence of paromomycin. Paromomycin alone did not cause a significant fluorescence change and did not affect the change in fluorescence when ternary complex bound to the IC. The fluorescent probe appears to be sensitive to both the codon recognition and domain closure events upon binding of ternary complex to the ribosome.

As described earlier, the first phase of the stopped-flow time courses contributed approximately 75% of the total fluorescence change in all reaction conditions tested. The second phase of the stopped-flow time courses contributed approximately 25% of the total fluorescence change. When ASL and paromomycin bound to the ribosome, approximately 70% of the total fluorescence change could be attributed to ASL binding alone and 30% could be attributed to the additional fluorescence change observed when ASL bound in the presence of paromomycin (Figure 5C). The correlation between the two phases of the stopped-flow time courses with the different fluorescence change observed when ASL binds

in the presence or absence of paromomycin indicates that in the stopped-flow time courses, the first phase corresponds to codon recognition and the second phase corresponds to domain closure. Assignment of the second phase to domain closure, however, needs to be validated by additional experiments.

GTP hydrolysis and peptidyl transfer

In order to measure the kinetics of GTP hydrolysis by ternary complex upon binding to the ribosome, ternary complexes containing [γ-^{32}P]GTP were mixed with IC in a quench flow instrument and the fraction of GTP hydrolyzed at each time point was determined by TLC and phosphorimaging (Figures S2A and S2B). Time courses of GTP hydrolysis were fit to a single exponential equation (Figure 6A). No second phase was evident in time courses of GTP hydrolysis, supporting the statement that the biphasic fluorescence time courses observed are due to a two step binding mechanism rather than subpopulations of less active ribosomes or ternary complex. Consistent with the fluorescence kinetics, the observed rates of GTP hydrolysis by ternary complex were faster in buffer B than A (Figure 6A). The rate of GTP hydrolysis by ternary complex was measured under increasing concentrations of IC in order to determine the saturation rate (Figure 6B). The rate of GTP hydrolysis was found to saturate at 12 s^{-1} in buffer A and 39 s^{-1} in buffer B (Table 3). Reported saturation rates of GTP hydrolysis vary widely in recent literature most likely due to the fact that typical concentration dependence measurements measure slightly more than half the saturation rate, requiring a large extrapolation of the data (25, 33, 48, 49). Our data reported here do agree well with previous studies performed under similar conditions (33, 49). Faster rates of GTP hydrolysis in buffer B supports the observation from the binding kinetics that physiological concentrations of polyamines can improve the efficiency of ternary complex binding to the ribosome. The rate of GTP hydrolysis in buffer A was slower and saturated earlier, indicating that the conformational change observed in the first phase of the stopped-flow time courses limits GTP hydrolysis under these conditions.

The rate of GTP hydrolysis in buffer A was found to saturate at a faster rate than the first phase of the fluorescence change from stopped-flow binding time courses. The faster observed rate is likely due to the lower NTP content in the GTP hydrolysis reactions. NTPs sequester Mg^{2+}, lowering the effective free Mg^{2+} content thus in the GTP hydrolysis experiments, the reactions occur in the presence of a greater effective Mg^{2+} concentration which would be expected to improve the binding step. Due to the differences in the reaction conditions, the rates measured in the GTP hydrolysis reactions cannot be directly compared to the binding kinetics. Nevertheless, it is clear that polyamines stimulate the rate of GTP hydrolysis when ternary complex reacts with ribosomes. It is likely that the stimulation in GTP hydrolysis occurs through improvements in the association of ternary complex to the ribosome rather than the chemistry step itself.

The kinetics of peptide bond formation were measured by mixing a 6-fold excess of ternary complex with IC containing [^{35}S]fMet-tRNA^{fMet} bound in the P-site in a quench flow instrument. Dipeptide products were separated by electrophoretic TLC and quantitated by phosphorimaging (Figures 6C, S2C and S2D). The observed rate of peptide bond formation was 9 ± 3 s^{-1} in buffer A and 10 ± 2 s^{-1} in buffer B, indicating that after the association of ternary complex to the ribosome, polyamines do not stimulate the rate of peptide bond formation (Table 3). One study showed that the rate of peptide bond formation may exhibit a significant concentration dependence (28). We therefore measured the rate of peptide bond formation at 2-fold lower concentration of ternary complex. The observed rate of peptide bond formation was found to be the same at the lower concentration of ternary complex, 9.3 ± 0.6 s^{-1} in buffer A and 8.4 ± 0.7 s^{-1} in buffer B.

Effect of polyamines on the fidelity of tRNA selection

Polyamines stimulate the rate of ternary complex association to the ribosome; however, studies on the effect of polyamines on the fidelity of protein synthesis have yielded conflicting results (43,50). In order to understand the effect of polyamines on the fidelity of protein synthesis, IC containing [^{35}S]fMet-tRNA^{fMet} in the P-site were mixed with ternary complexes formed from total tRNA mixtures. The reactions were quenched after 30 seconds and the products were separated by electrophoretic TLC (Figure 7A). The amount of correct and incorrect dipeptide formed under all buffer conditions was quantitated by phosphorimaging. The observed fractions of incorrect dipeptide formed were 0.04 ± 0.01 in buffer A, 0.026 ± 0.004 in buffer B, 0.027 ± 0.007 in buffer C, and 0.081 ± 0.004 in buffer D (Figure 7B). Consistent with previous work, magnesium was found to decrease the fidelity of protein synthesis. Slightly lower misincorporation was observed in the case of buffers with physiological polyamine content (buffers B and C) when compared to the low Mg^{2+}/polyamine buffer (buffer A). Unlike Mg^{2+}, polyamines are able to significantly stimulate the binding of ternary complex to the ribosome without decreasing the fidelity of protein synthesis.

Discussion

We have developed a new fluorescence based assay to monitor the binding of ternary complex to the ribosome. An increase in the fluorescence intensity of pyrene covalently attached to the 3' end of a short mRNA occurs when ternary complex binds to the A-site. The observed increase in fluorescence is independent of GTP hydrolysis by EF-Tu and shows biphasic kinetics. The first phase is correlated with codon recognition as shown by experiments with ASL (Figure 2D). The second phase is attributed to domain closure as judged by experiments with ASL and paromomycin (Figures 5B and 5C). Binding of ASL with paromomycin to the A-site results in the same fluorescence change observed when full length tRNAs bind. This is consistent with observations from crystallography that domain closure is enhanced when the cognate ASL binds in the presence of the miscoding antibiotic paromomycin (7). The new assay for monitoring the pre-steady state kinetics of the binding of ternary complex to the ribosome can be used with any tRNA or tRNA transcript. This opens up the possibility for examining the process of tRNA selection with tRNAs having various substitutions.

Details of the mechanism of ternary complex association to the ribosome measured here have significant implications for our understanding of decoding. The current kinetic model of ternary complex binding to the ribosome has been determined primarily through one fluorescence method (13). One step in the current model of tRNA selection by the ribosome that has been controversial is the “initial binding” step (Figure 1). It is proposed that prior to codon recognition, the ternary complex binds to the ribosome in a non-specific initial binding complex (15). In this model, cognate, near-cognate, and non-cognate ternary complexes appear to all bind equivalently. A non-specific initial binding mode would be expected to inhibit protein synthesis by competitive inhibition of cognate ternary complexes (16). Additionally, the kinetics of the transition of non-cognate ternary complex from initial binding to codon recognition indicates that an incorrect ternary complex would be passed between these two binding conformations many times prior to dissociation of the ternary complex, further inhibiting protein synthesis (17). Experiments directly measuring the inhibition of protein synthesis by near-cognate ternary complex have shown that no such inhibition occurs indicating that nonspecific binding of ternary complexes is negligible (51).

According to our kinetic results, codon recognition occurs as a second-order process, indicating that there is no initial binding step, or that transition from initial binding to codon recognition is extremely fast, allowing codon recognition to display apparent second-order

kinetics. Under compromised conditions, we see codon recognition occurs as a conformational change, indicating that there may be an initial binding step that is only apparent under suboptimal conditions. Rapid entry of ternary complex either directly into the codon recognition step or via a pathway that does not allow the observation of an initial binding intermediate explains why incorrect ternary complexes do not inhibit protein synthesis.

Our studies with polyamines showed that spermine and spermidine allowed the codon recognition step to occur as a second-order process and stimulated the association of ternary complex to the ribosome at least as well or better than 20 mM Mg^{2+}. The rate of the second phase of the stopped-flow time courses of ternary complex binding was also stimulated equally well by polyamines or Mg^{2+}. The relatively slow saturation rate of the second phase from stopped-flow time courses suggests that domain closure occurs as a late event in ternary complex binding to the ribosome and may be important in positioning the tRNA in the A-site for peptidyl transfer during the accommodation step. Alternatively, the second phase may represent a conformational change in the ribosome that occurs after domain closure.

The stimulation of ternary complex binding to the ribosome by polyamines was confirmed by measuring the rate of GTP hydrolysis by EF-Tu. Spermine stimulated the rate of GTP hydrolysis by ternary complex. At low concentrations of spermidine and Mg^{2+}, GTP hydrolysis appears to be rate limited by the preceding codon recognition step, which is severely inhibited under these conditions. Peptidyl transfer reactions showed identical kinetics in buffers A and B indicating that after the association of ternary complex to the ribosome, polyamines do not significantly stimulate forward reactions. Additionally, fidelity measurements showed that the polyamines spermine and spermidine do not decrease the fidelity of protein synthesis, unlike Mg^{2+}, which has been shown to significantly reduce the fidelity of decoding (14,43).

Polyamines bind to tRNAs and influence the structure of the anticodon loop as has been shown by crystallography (22), limited RNase digestion (52), fluorescence (23), and photocrosslinking studies (53). Electron density difference maps showed that spermine binds to the anticodon stem of $tRNA^{Phe}$ in the hinge region (22) that must adopt an “untwisted”, “kinked” intermediate when the tRNA adopts the A/T state prior to GTP hydrolysis by EF-Tu (4). This region has functionally been shown to be vital for the correct decoding of tRNAs by the ribosome (48). While it has long been known that polyamines stimulate protein synthesis, the mechanism of this stimulation has remained largely unknown (44). Here, we have shown that the polyamines spermine and spermidine are able to greatly stimulate the association of ternary complex to the ribosome at physiological concentrations with relatively low Mg^{2+} concentration without compromising fidelity.

Supplementary Material

Refer to Web version on PubMed Central for supplementary material.

Acknowledgments

We thank Jack Kyte for discussions and Ulrich Muller for comments on the manuscript.

This work was supported by National Institutes of Health (NIH) Molecular Biophysics Training Grant GM08326 and NIH Training Program in Hemoglobin and Blood Protein Chemistry Grant 5T32-DK007233 to B.H. and NIH Grant GM065265 to S.J.

Abbreviations

EF-Tu	elongation factor Tu
rRNA	ribosomal RNA
mRNA	messenger RNA
tRNA	transfer RNA

References

1. Edelmann P, Gallant J. Mistranslation in E. coli. Cell. 1977; 10:131–137. [PubMed: 138485]
2. Bouadloun F, Donner D, Kurland CG. Codon-specific missense errors in vivo. Embo J. 1983; 2:1351–1356. [PubMed: 10872330]
3. Ogle JM, Brodersen DE, Clemons WM Jr. Tarry MJ, Carter AP, Ramakrishnan V. Recognition of cognate transfer RNA by the 30S ribosomal subunit. Science. 2001; 292:897–902. [PubMed: 11340196]
4. Schmeing TM, Voorhees RM, Kelley AC, Gao YG, Murphy F. V. t. Weir JR, Ramakrishnan V. The crystal structure of the ribosome bound to EF-Tu and aminoacyltRNA. Science. 2009; 326:688–694. [PubMed: 19833920]
5. Selmer M, Dunham CM, Murphy F. V. t. Weixlbaumer A, Petry S, Kelley AC, Weir JR, Ramakrishnan V. Structure of the 70S ribosome complexed with mRNA and tRNA. Science. 2006; 313:1935–1942. [PubMed: 16959973]
6. Korostelev A, Trakhanov S, Laurberg M, Noller HF. Crystal structure of a 70S ribosome-tRNA complex reveals functional interactions and rearrangements. Cell. 2006; 126:1065–1077. [PubMed: 16962654]
7. Ogle JM, Murphy FV, Tarry MJ, Ramakrishnan V. Selection of tRNA by the ribosome requires a transition from an open to a closed form. Cell. 2002; 111:721–732. [PubMed: 12464183]
8. Hopfield JJ. Kinetic proofreading: a new mechanism for reducing errors in biosynthetic processes requiring high specificity. Proc Natl Acad Sci U S A. 1974; 71:4135–4139. [PubMed: 4530290]
9. Ninio J. Kinetic amplification of enzyme discrimination. Biochimie. 1975; 57:587–595. [PubMed: 1182215]
10. Thompson RC, Stone PJ. Proofreading of the codon-anticodon interaction on ribosomes. Proc Natl Acad Sci U S A. 1977; 74:198–202. [PubMed: 319457]
11. Thomposon RC, Dix DB. Accuracy of protein biosynthesis. A kinetic study of the reaction of poly(U)-programmed ribosomes with a leucyl-tRNA2-elongation factor Tu-GTP complex. J Biol Chem. 1982; 257:6677–6682. [PubMed: 6919538]
12. Thompson RC, Karim AM. The accuracy of protein biosynthesis is limited by its speed: high fidelity selection by ribosomes of aminoacyl-tRNA ternary complexes containing GTP[gamma S]. Proc Natl Acad Sci U S A. 1982; 79:4922–4926. [PubMed: 6750613]
13. Pape T, Wintermeyer W, Rodnina MV. Complete kinetic mechanism of elongation factor Tu-dependent binding of aminoacyl-tRNA to the A site of the E. coli ribosome. EMBO J. 1998; 17:7490–7497. [PubMed: 9857203]
14. Pape T, Wintermeyer W, Rodnina M. Induced fit in initial selection and proofreading of aminoacyl-tRNA on the ribosome. Embo J. 1999; 18:3800–3807. [PubMed: 10393195]
15. Rodnina MV, Pape T, Fricke R, Kuhn L, Wintermeyer W. Initial binding of the elongation factor Tu.GTP.aminoacyl-tRNA complex preceding codon recognition on the ribosome. J Biol Chem. 1996; 271:646–652. [PubMed: 8557669]
16. Johansson M, Lovmar M, Ehrenberg M. Rate and accuracy of bacterial protein synthesis revisited. Curr Opin Microbiol. 2008; 11:141–147. [PubMed: 18400551]
17. Ninio J. Multiple stages in codon-anticodon recognition: double-trigger mechanisms and geometric constraints. Biochimie. 2006; 88:963–992. [PubMed: 16843583]
18. Blanchard SC, Gonzalez RL, Kim HD, Chu S, Puglisi JD. tRNA selection and kinetic proofreading in translation. Nat Struct Mol Biol. 2004; 11:1008–1014. [PubMed: 15448679]

19. Lee TH, Blanchard SC, Kim HD, Puglisi JD, Chu S. The role of fluctuations in tRNA selection by the ribosome. Proc Natl Acad Sci U S A. 2007; 104:13661–13665. [PubMed: 17699629]
20. Blanchard SC, Kim HD, Gonzalez RL Jr. Puglisi JD, Chu S. tRNA dynamics on the ribosome during translation. Proc Natl Acad Sci U S A. 2004; 101:12893–12898. [PubMed: 15317937]
21. Geggier P, Dave R, Feldman MB, Terry DS, Altman RB, Munro JB, Blanchard SC. Conformational Sampling of Aminoacyl-tRNA during Selection on the Bacterial Ribosome. J Mol Biol. 2010; 399:576–595. [PubMed: 20434456]
22. Quigley GJ, Teeter MM, Rich A. Structural analysis of spermine and magnesium ion binding to yeast phenylalanine transfer RNA. Proc Natl Acad Sci U S A. 1978; 75:64–68. [PubMed: 343112]
23. Nilsson L, Rigler R, Wintermeyer W. The influence of spermine on the structural dynamics of yeast tRNAPhe. Biochim Biophys Acta. 1983; 740:460–465. [PubMed: 6349691]
24. Bartetzko A, Nierhaus KH. Mg2+/NH4+/polyamine system for polyuridine-dependent polyphenylalanine synthesis with near in vivo characteristics. Methods Enzymol. 1988; 164:650–658. [PubMed: 3071686]
25. Gromadski KB, Rodnina MV. Kinetic determinants of high-fidelity tRNA discrimination on the ribosome. Mol Cell. 2004; 13:191–200. [PubMed: 14759365]
26. Gromadski KB, Daviter T, Rodnina MV. A uniform response to mismatches in codon-anticodon complexes ensures ribosomal fidelity. Mol Cell. 2006; 21:369–377. [PubMed: 16455492]
27. Powers T, Noller HF. A functional pseudoknot in 16S ribosomal RNA. EMBO J. 1991; 10:2203–2214. [PubMed: 1712293]
28. Johansson M, Bouakaz E, Lovmar M, Ehrenberg M. The kinetics of ribosomal peptidyl transfer revisited. Mol Cell. 2008; 30:589–598. [PubMed: 18538657]
29. Studer SM, Feinberg JS, Joseph S. Rapid Kinetic Analysis of EF-G-dependent mRNA Translocation in the Ribosome. J Mol Biol. 2003; 327:369–381. [PubMed: 12628244]
30. Meinnel T, Blanquet S. Maturation of pre-tRNA(fMet) by Escherichia coli RNase P is specified by a guanosine of the 5'-flanking sequence. J Biol Chem. 1995; 270:15908–15914. [PubMed: 7797595]
31. Feinberg JS, Joseph S. Ribose 2'-hydroxyl groups in the 5' strand of the acceptor arm of P-site tRNA are not essential for EF-G catalyzed translocation. RNA. 2006; 12:580–588. [PubMed: 16489185]
32. Bilgin N, Ehrenberg M, Ebel C, Zaccai G, Sayers Z, Koch MH, Svergun DI, Barberato C, Volkov V, Nissen P, Nyborg J. Solution structure of the ternary complex between aminoacyl-tRNA, elongation factor Tu, and guanosine triphosphate. Biochemistry. 1998; 37:8163–8172. [PubMed: 9609712]
33. Pan D, Zhang CM, Kirillov S, Hou YM, Cooperman BS. Perturbation of the tRNA tertiary core differentially affects specific steps of the elongation cycle. J Biol Chem. 2008; 283:18431–18440. [PubMed: 18448426]
34. Studer SM, Joseph S. Unfolding of mRNA secondary structure by the bacterial translation initiation complex. Mol Cell. 2006; 22:105–115. [PubMed: 16600874]
35. Hetrick B, Lee K, Joseph S. Kinetics of stop codon recognition by release factor 1. Biochemistry. 2009; 48:11178–11184. [PubMed: 19874047]
36. Yusupova G, Jenner L, Rees B, Moras D, Yusupov M. Structural basis for messenger RNA movement on the ribosome. Nature. 2006; 444:391–394. [PubMed: 17051149]
37. Scarano G, Krab IM, Bocchini V, Parmeggiani A. Relevance of histidine-84 in the elongation factor Tu GTPase activity and in poly(Phe) synthesis: its substitution by glutamine and alanine. FEBS Lett. 1995; 365:214–218. [PubMed: 7781781]
38. Daviter T, Wieden HJ, Rodnina MV. Essential role of histidine 84 in elongation factor Tu for the chemical step of GTP hydrolysis on the ribosome. J Mol Biol. 2003; 332:689–699. [PubMed: 12963376]
39. Igarashi K, Sugawara K, Izumi I, Nagayama C, Hirose S. Effect of polyamines of polyphenylalanine synthesis by Escherichia coli and rat-liver ribosomes. Eur J Biochem. 1974; 48:495–502. [PubMed: 4614977]
40. Lamborg MR, Zamecnik PC. Amino acid incorporation into protein by extracts of E. coli. Biochim Biophys Acta. 1960; 42:206–211. [PubMed: 13758500]

41. Tissieres A, Schlessinger D, Gros F. Amino Acid Incorporation into Proteins by Escherichia Coli Ribosomes. Proc Natl Acad Sci U S A. 1960; 46:1450–1463. [PubMed: 16590771]
42. Nathans D, Lipmann F. Amino acid transfer from aminoacyl-ribonucleic acids to protein on ribosomes of Escherichia coli. Proc Natl Acad Sci U S A. 1961; 47:497–504. [PubMed: 13727926]
43. Thompson RC, Dix DB, Gerson RB, Karim AM. Effect of Mg2+ concentration, polyamines, streptomycin, and mutations in ribosomal proteins on the accuracy of the two-step selection of aminoacyl-tRNAs in protein biosynthesis. J Biol Chem. 1981; 256:6676–6681. [PubMed: 6113247]
44. Igarashi K, Kashiwagi K. Polyamines: mysterious modulators of cellular functions. Biochem Biophys Res Commun. 2000; 271:559–564. [PubMed: 10814501]
45. Johnson KA. Rapid kinetic analysis of mechanochemical adenosinetriphosphatases. Methods Enzymol. 1986; 134:677–705. [PubMed: 2950300]
46. Johnson, KA. Transient-state kinetic analysis of enzyme reaction pathways. In: Sigman, DS., editor. The Enzymes. Academic Press, Inc.; New York: 1992. p. 1-61.
47. Fierke CA, Johnson KA, Benkovic SJ. Construction and evaluation of the kinetic scheme associated with dihydrofolate reductase from Escherichia coli. Biochemistry. 1987; 26:4085–4092. [PubMed: 3307916]
48. Cochella L, Green R. An active role for tRNA in decoding beyond codon:anticodon pairing. Science. 2005; 308:1178–1180. [PubMed: 15905403]
49. Ledoux S, Olejniczak M, Uhlenbeck OC. A sequence element that tunes Escherichia coli tRNA(Ala)(GGC) to ensure accurate decoding. Nat Struct Mol Biol. 2009; 16:359–364. [PubMed: 19305403]
50. Ito K, Igarashi K. The increase by spermidine of fidelity of protamine synthesis in a wheat-germ cell-free system. Eur J Biochem. 1986; 156:505–510. [PubMed: 3084256]
51. Bilgin N, Ehrenberg M, Kurland C. Is translation inhibited by noncognate ternary complexes? FEBS Lett. 1988; 233:95–99. [PubMed: 2454844]
52. Peng Z, Kusama-Eguchi K, Watanabe S, Ito K, Watanabe K, Nomoto Y, Igarashi K. Responsibility of tRNA(Ile) for spermine stimulation of rat liver Ile-tRNA formation. Arch Biochem Biophys. 1990; 279:138–145. [PubMed: 2337346]
53. Amarantos I, Kalpaxis DL. Photoaffinity polyamines: interactions with AcPhetRNA free in solution or bound at the P-site of Escherichia coli ribosomes. Nucleic Acids Res. 2000; 28:3733–3742. [PubMed: 11000265]

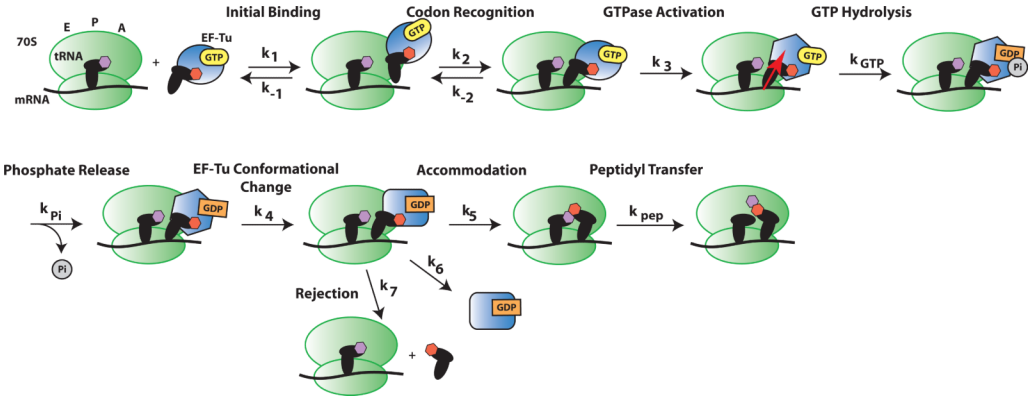

Figure 1. The kinetic steps in tRNA selection

The top row represents initial selection and the bottom row represents proofreading by the ribosome. Ribosomes are represented in green, EF-Tu is indicated in blue, aminoacyl-tRNA is indicated in black, GTP is indicated in yellow, GDP is indicated in orange. The steps in tRNA selection are: initial binding (k_1, k_{-1}), codon recognition (k_2, k_{-2}), GTPase activation (k_3), GTP hydrolysis (k_{GTP}), phosphate release (k_{Pi}), EF-Tu conformational change (k_4), accommodation (k_5), dissociation of EF-Tu•GDP (k_6), rejection of aminoacyl-tRNA (k_7), and peptide bond formation (k_{pep}) (13,14,25).

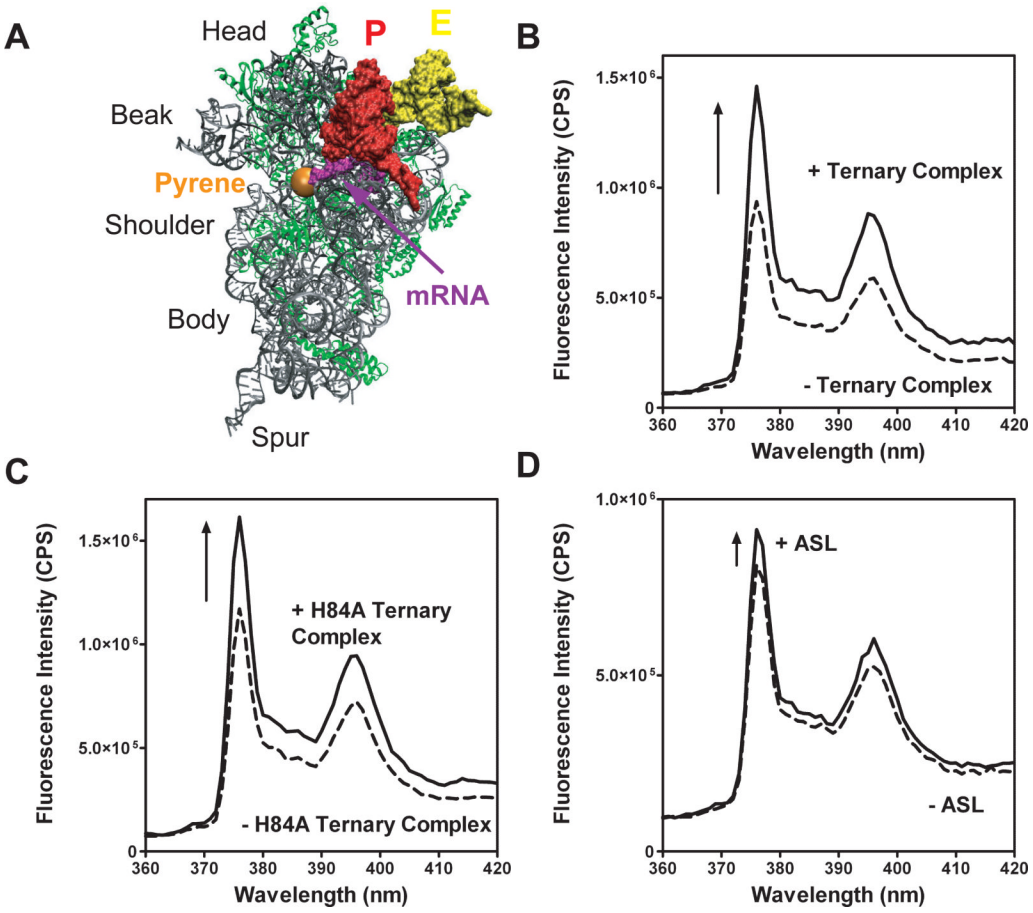

Figure 2. Fluorescence-based assay to monitor tRNA binding to the ribosome

(A) Approximate location of the pyrene probe (orange) attached to the 3' end of a short model mRNA in the 30S subunit. 16S rRNA (gray) small subunit proteins (green), P-site tRNA (red), E-site tRNA (yellow), mRNA (purple). (B) Addition of 1 μM ternary complex to 0.25 μM fluorescently labeled initiation complex (IC) results in an increase in fluorescence of the pyrene probe. Fluorescence emission profile before addition of ternay complex (dashed line) and after (solid line) are shown. Fluorescence intensity is in counts per second (CPS). (C) Addition of ternary complex containing GTPase deficient H84A EF-Tu results in an equivalent fluorescence change. (D) Addition of 20 μM ASL to fluorescently labeled IC results in a smaller increase in fluorescence.

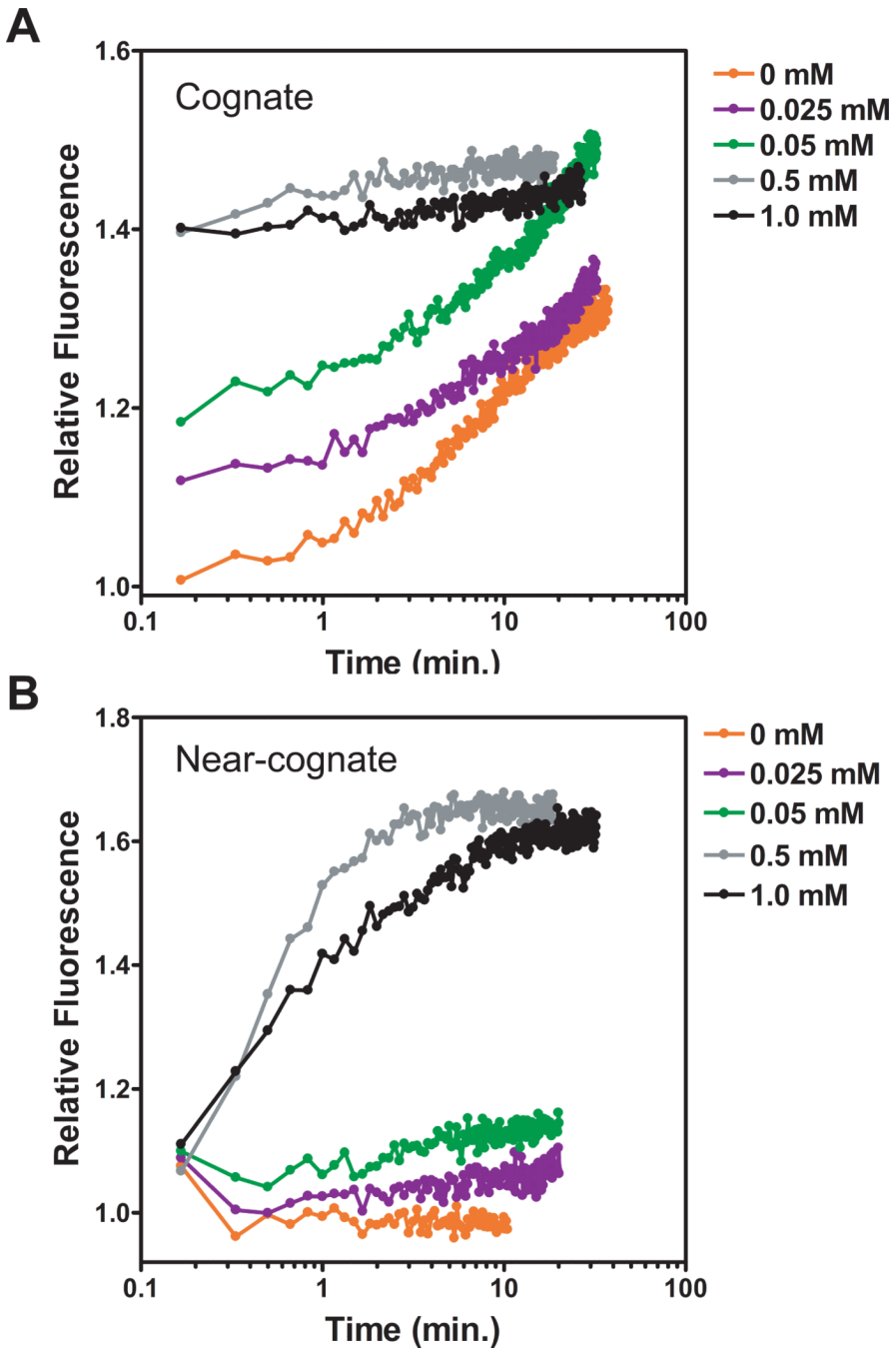

Figure 3. Effect of spermine on the binding of tRNAs to the ribosome

(A) 0.25 μM IC programmed with a cognate UUU codon in the A-site were mixed with 1 μM $tRNA^{Phe}$ containing ternary complex and the relative fluorescence is reported over time in buffers containing increasing concentrations of spermine. (B) Fluorescence change upon mixing ternary complex with fluorescently labeled IC programmed with the near-cognate codon CUC in the A-site. Relative fluorescence is determined by dividing all data points by the fluorescence intensity of IC before addition of ternary complex.

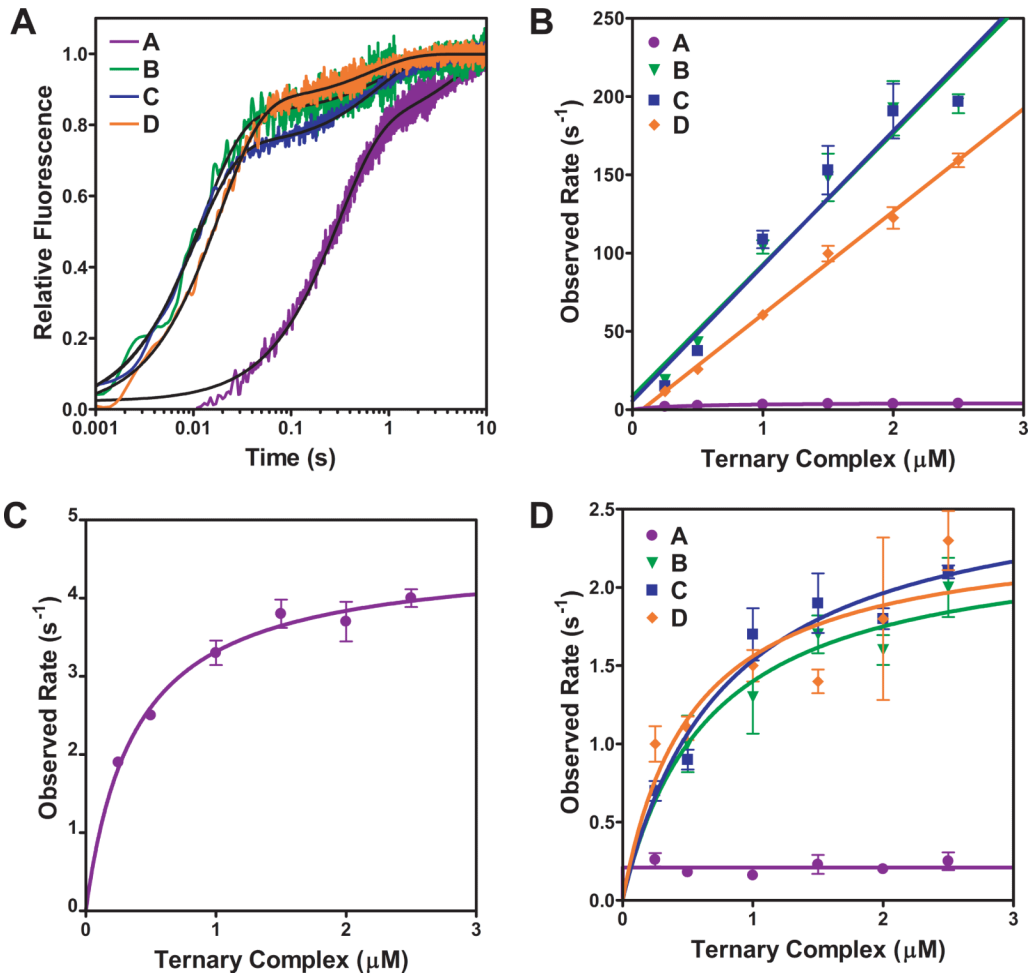

Figure 4. Kinetics of ternary complex binding to the ribosome

(A) Representative time courses showing the binding of ternary complex to the ribosome in the indicated buffers (0.25 μM IC was mixed with 1 μM ternary complex). Data were fit to the sum of two exponential equations (black line). (B) Concentration dependence of the first phase of the time courses. The concentration dependence curve was fit to a linear equation in the case of buffers B, C, and D. A hyperbolic equation was used to fit the concentration dependence curve in buffer A. (C) Concentration dependence of the first phase of the time course in buffer A (blown up from B). (D) Concentration dependence of the second phase of the time courses in all buffers was fit to a hyperbolic equation. In all cases, the standard deviations from two to three independent experiments are indicated.

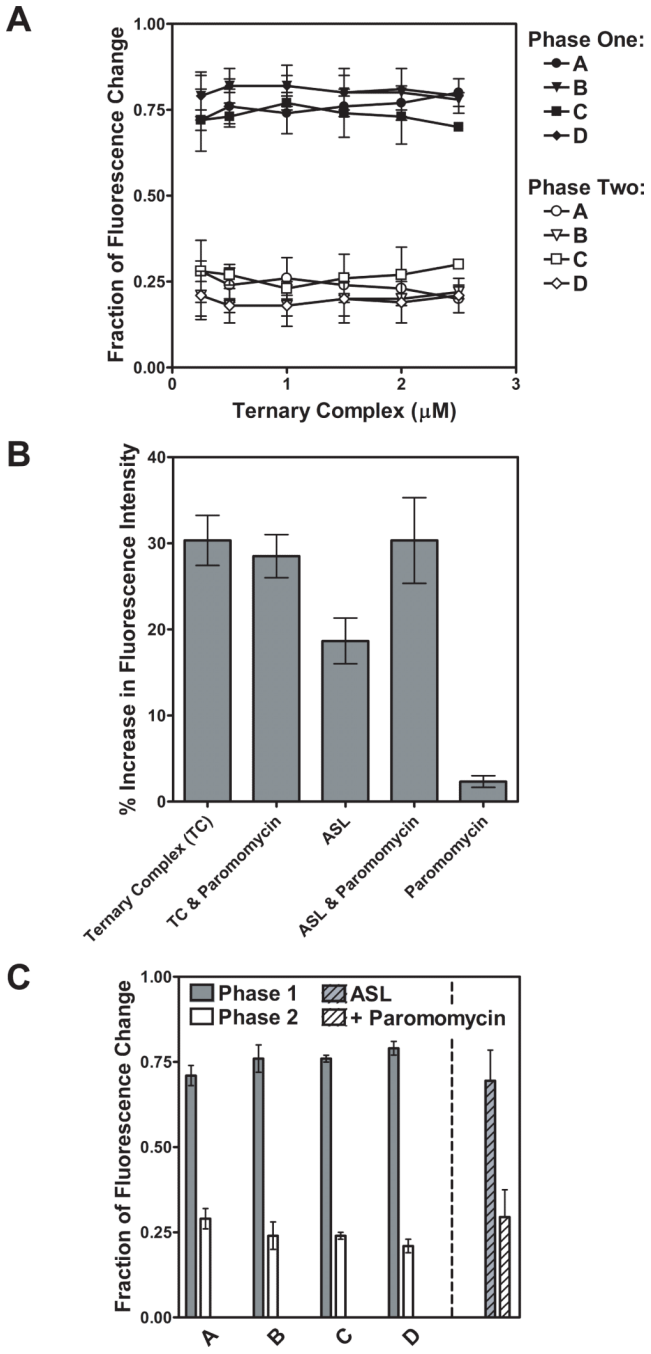

Figure 5. Analysis of biphasic fluorescence change

(A) Concentration dependence of the amplitudes of each phase of the fluorescence change. Under all conditions and concentrations tested, the first phase of the fluorescence change contributed approximately 75% of the total fluorescence change and the second phase contributed approximately 25%. (B) Percent increase in fluorescence shown when ternary complex (TC), TC and paromomycin, ASL, ASL and paromomycin, or paromomycin alone were mixed with fluorescently labeled IC. (C) The fraction of the fluorescence change contributed by phase one (gray bars) and phase two (white bars) in all buffers tested is compared to the fluorescence change observed when ASL alone (gray bar with lines) binds

to the ribosome or the additional fluorescence change when ASL is added in the presence of paromomycin (white bar with lines).

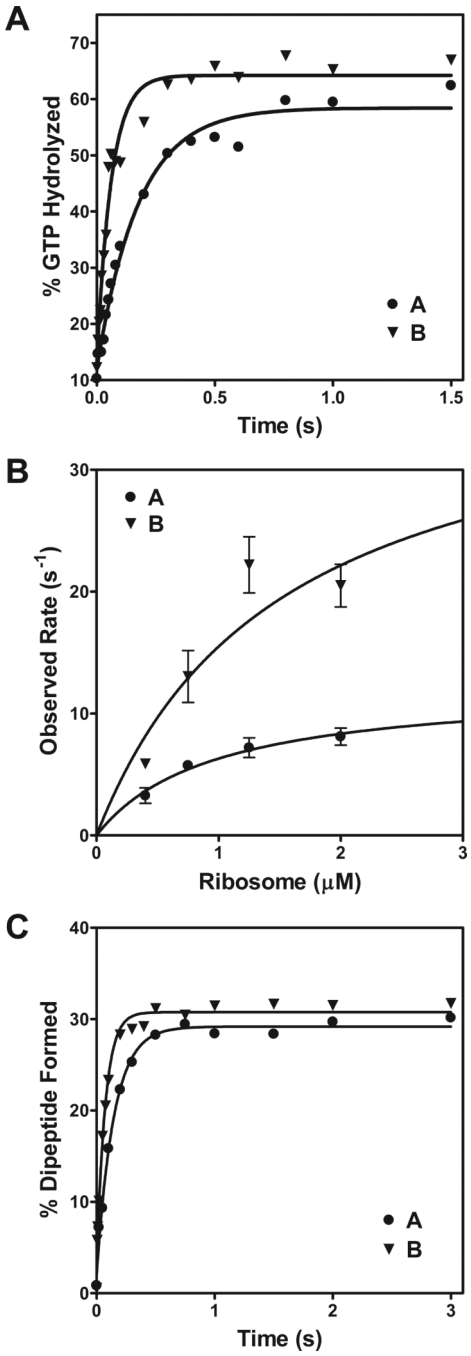

Figure 6. Kinetics of GTP hydrolysis and peptidyl transfer

(A) Time course of GTP hydrolysis reaction when 0.25 μM ternary complex containing [γ^{32}P]GTP is mixed with 0.75 μM IC in buffer A (•) or buffer B (▼). Data were fit to a single exponential equation. (B) Concentration dependence of the observed rate of GTP hydrolysis at varying concentrations of IC. Saturation rates of GTP hydrolysis were determined by fitting to a hyperbolic equation. The standard deviations from two to three independent experiments are indicated. (C) Time course of [^{35}S]fMet-Phe dipeptide formed when 1.5 μM ternary complex is mixed with IC containing [^{35}S]fMet-tRNA^{fMet} in the P-site. Data were fit to a single exponential equation.

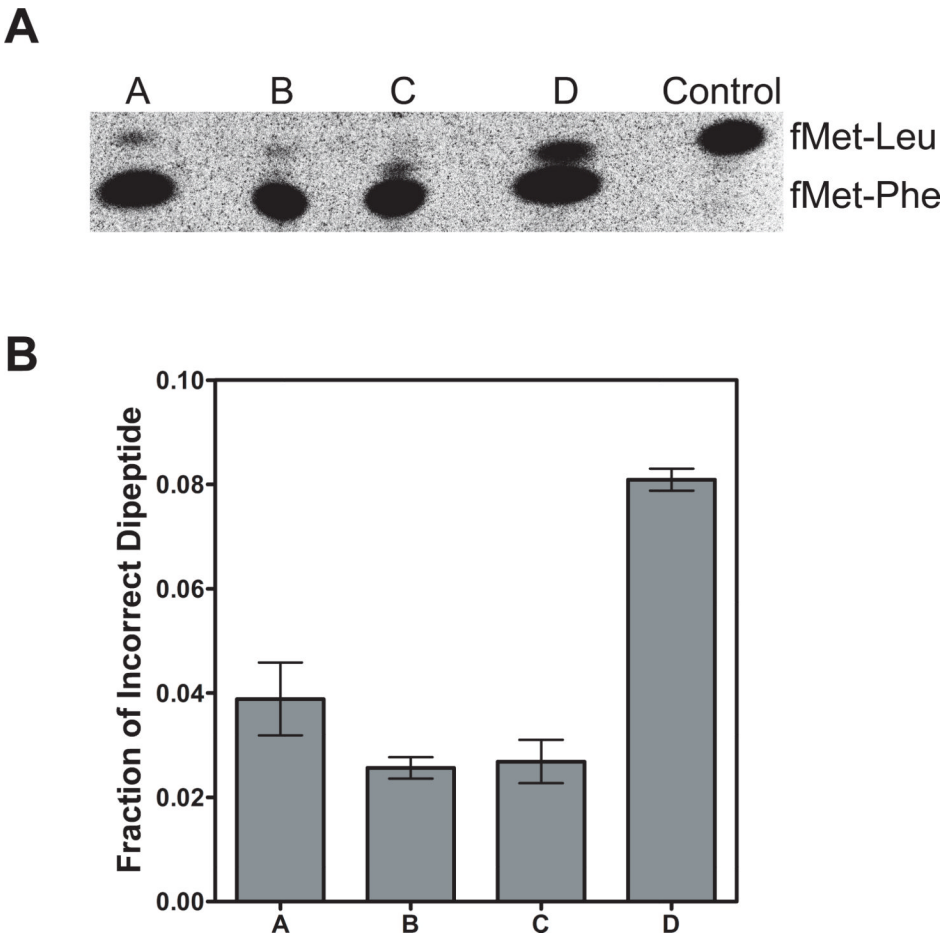

Figure 7. Effect of polyamines on the fidelity of tRNA selection

(A) A representative electrophoretic TLC showing the products of the fidelity experiment in the four buffer systems. IC containing [^{35}S]fMet-tRNA^{fMet} in the P site and UUU codon in the A site was mixed with ternary complex formed from total tRNA mixtures. A control reaction with CUC codon in the A site was performed in parallel to serve as a marker for [^{35}S]fMet-Leu dipeptide. Only two product spots were observed. One spot corresponds to the cognate [^{35}S]fMet-Phe dipeptide, the other spot corresponds to the near-cognate [^{35}S]fMet-Leu dipeptide. (B) Bar graph showing the fraction of incorrect [^{35}S]fMet-Leu dipeptide formed in each buffer system.

Table 1

Polyamine and Mg^{2+} concentration in each buffer and in vivo

Buffer	Spermine (mM)	Spermidine (mM)	Putrescine (mM)	Mg^{2+} (mM)
A	-	0.5	8	3.5
B	0.5	-	8	3.5
C	-	5	8	3.5
D	-	-	-	20
In vivo	1	7	32	0.5-1[a]

[a] Free Mg^{2+}

Table 2

Rate constants for ternary complex binding to the ribosome

Buffer	k_{on} (μM^{-1} s^{-1})	k_{max1} (s^{-1})	k_{max2} (s^{-1})
A	-	5	0.2
B	84	-	2.3
C	86	-	2.7
D	66	-	2.4

Table 3

Rate constants for GTP hydrolysis and peptidyl transfer

Buffer	k_{GTP} (s^{-1})	k_{pep} (s^{-1})
A	12	9 ± 3
B	39	10 ± 2